

Controlling J-coupling evolution during selective RF pulses

L. Mitschang¹

¹Medical Physics and Metrological Information Technology, Physikalisch-Technische Bundesanstalt, Berlin, Berlin, Germany

Introduction

MR relies on the ability to manipulate spin systems through well defined rotations by RF pulses and evolution of the coupling network. As long as pulses are short in comparison to the inverse of the coupling strength, both modalities may be applied independently in a building-block manner. For longer pulses, as are used e.g. for spectral or spatial frequency selectivity, however, the effects of J-coupling and RF irradiation are intertwined. The design as well as the interpretation of experiments are no longer straightforward and have to be augmented by precise calculations of spin evolution. We present a theoretical analysis which shows that the interference of RF and J-coupling can be disentangled in a manner similar to the short pulse limit for a number of well-known frequency selective RF pulses. The case study is polarization transfer through INEPT (Insensitive Nuclei Enhanced by Polarization Transfer [1]), a technique used for signal enhancement, editing, and correlation spectroscopy in in-vivo MRI and MRS.

Methods

Consider the INEPT element in Fig. 1 applied to a heteronuclear pair of spin-1/2 I and S, weakly scalar coupled with strength J. A shaped pulse is used to invert spin S frequency selectively. Were a short, non-selective π -pulse used instead to flip S instantaneously, the sequence could be analysed easily [1]: the excitation pulse generates $-\gamma_I I_Y + \gamma_S S_Z$ from thermal equilibrium; chemical shift evolution is refocused by the synchronously applied π -pulses; thus, only J-coupling prevails in both δ -periods; the state of the spin system prior to the final pulse pair is $-\gamma_I I_Y \cos(\pi J 2\delta) + \gamma_I 2I_X S_Z \sin(\pi J 2\delta) - \gamma_S S_Z$; the final pair of synchronous $\pi/2$ -pulses achieves the polarization transfer by converting spin I anti-phase $\gamma_I 2I_X S_Z \sin(\pi J 2\delta)$ to spin S anti-phase of spin I sensitivity $\gamma_I 2I_Z S_Y \sin(\pi J 2\delta)$ (which evolves further, e.g. to spin S magnetization for detection); ignoring relaxation, optimum signal is obtained for $\delta = 1/4J$. The duration of selective inversion pulses is in the ms range which is on the order of $1/J$ for the common 1-bond pairs 1H-13C and 1H-15N. As a consequence of the interference of RF with J-coupling, in-phase I_Y and anti-phase $2I_X S_Z$ do not exchange exclusively (as during free evolution periods δ) but are in addition converted to zero and double quantum coherence $2I_X S_Y$ in a rather complex manner. For INEPT without free evolution periods ($\delta = 0$), the amount of $2I_X S_Y$ present at the end of selective pulses RE-BURP (R) [2], I-BURP-2 (I) [2], Gaussian pulse truncated at 1% of the peak RF amplitude (G) [3], rectangular pulse (H), and Gaussian cascade (G3) [4], in dependence of the pulse length is shown in Fig. 2. The pulses are applied on-resonance and the area is calibrated to achieve a perfect π -rotation of an isolated spin S for any pulse length used in the simulation (100 μ s to 10 ms in 100 μ s steps); having 1H-13C in mind, the coupling is set to $J = 138.8$ Hz. For clarity of presentation, only in case of R is the amplitude of in-phase and anti-phase also included in Fig. 2. Evidently, both coherences exchange almost perfectly harmonically which is due to a nearly vanishing perturbation $2I_X S_Y$. The result also occurs when in-phase and anti-phase have already exchanged before application of a pulse because of a finite δ -period. Similar behaviour (data not shown) is found for I, G, and H where again only weak $2I_X S_Y$ is present. These findings suggest the modelling of the action of selective pulses R, I, G, and H in INEPT as spin inverting (refocusing chemical shift) and, additionally but independently, as facilitating the evolution $I_Y \cos(\pi J_{\text{eff}} \tau) + 2I_X S_Z \sin(\pi J_{\text{eff}} \tau)$ with an effective coupling constant J_{eff} for the duration τ of the pulse. G3 fails to obey the model because of to strongly growing zero and double quantum coherences.

Results and Discussion

For R, I, G, and H pulses of any length within the range 100 μ s to 2 ms of the simulation, J_{eff} is determined from the calculated anti-phase amplitude A as $\arcsin(A)/\pi$ and from these values the mean effective coupling constant \bar{J} is formed. The attenuation $r = \bar{J}/J$ in coupling strength is 0.951, 0.312, 0.831, and 0.636 for R, I, G, and H, respectively. These values are rather universal in practical terms, even though derived for a specific $J = 138.8$ Hz. Fig. 3 shows the absolute difference between the true anti-phase amplitude and $\sin(\pi J \tau)$ for common pulse lengths (0 to 10 ms) and coupling strengths (0 to 200 Hz) for I, G, and H. For most of the domain, the error is less than a hundredth (for R the error is below 0.008 in the total domain considered). Particularly the validity of the model for small J indicates its applicability to homonuclear 1H MRS, as long as the protons are weakly coupled. Our results do not depend critically on the chosen range of pulse lengths and coupling strengths to determine \bar{J} (and thus r), as long as the perturbation $2I_X S_Y$ is sufficiently small. Further pulse shapes may be analysed along the same lines as the possibility to dissolve their action into a well defined rotation and an independently effective J-coupling evolution eases their optimum use in INEPT and related experiments.

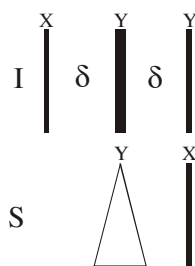


Fig. 1: INEPT element with thin (thick) solid bars for $\pi/2$ (π) pulses, open triangle for selective pulse. Phases are indicated.

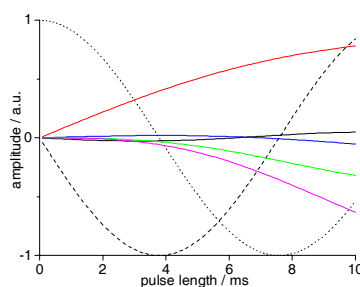


Fig. 2: Amplitude of $2I_X S_Y$ for R (black), I (blue), G (green), H (magenta), and G3 (red), amplitudes of I_Y (dotted) and $2I_X S_Z$ (dashed) for R in dependence of duration of pulse.

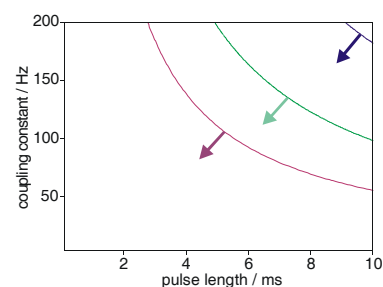


Fig. 3: Contours of 0.01 for absolute difference of anti-phase amplitude and $\sin(\pi J \tau)$ for I (blue), G (green), and H (magenta). Arrows indicate regions of error below 0.01.

References

- [1] De Graaf R. A., *In vivo NMR spectroscopy*, Wiley, NY, 1998. [2] Geen H., et al. *J. Magn. Reson.* **93**; 93 (1991). [3] Bauer C., et al., *J. Magn. Reson.* **58**, 442 (1984). [4] Emsley L., et al., *Chem. Phys. Lett.* **165** (6), 469 (1990).